

A SPLITTING INTEGRATOR FOR THE BCS EQUATIONS OF SUPERCONDUCTIVITY

J. SEYRICH[†]

Abstract. The BCS equations are the centerpiece of the microscopic description of superconductivity. Their space discretization yields a system of coupled ordinary differential equations. For the physically important case of the BCS equations for a contact interaction potential, we come up with a fast time evolution scheme based on a splitting approach which only requires basic operations. The computational cost of the scheme grows only linearly with the dimension of the space discretization. Its accuracy is demonstrated in extensive numerical experiments. These experiments also show that the physical energy of the system is preserved up to very small errors.

Key words. coupled differential equations, time discretization, splitting methods, fast algorithm, conservation of first integrals

Introduction. In this work, we consider the time-dependent BCS equations for a translation invariant system, given by

$$i \frac{\partial \gamma(t, x)}{\partial t} = -2 \int_{\mathbb{R}} V(y) \operatorname{Im} \left[\alpha(t, x - y) \overline{\alpha(t, y)} \right] dy, \quad (0.1)$$

$$i \frac{\partial \alpha(t, x)}{\partial t} = 2 \left(-\frac{d^2}{dx^2} - \mu + V(x) \right) \alpha(t, x) - 4 \int_{\mathbb{R}} \gamma(t, x - y) V(y) \alpha(t, y) dy, \quad (0.2)$$

where a and μ are positive, real-valued parameters and the bar denotes complex conjugation. These equations, named after *Bardeen, Cooper and Schrieffer*, see [1], are the basis of the microscopic description of superconductivity in metals. They describe the evolution of the particle density γ and the Cooper pair density α . We refer the interested reader to [2] for a detailed introduction.

Equation (0.2) resembles the linear Schrödinger equation for quantum dynamical systems. One important aspect of these systems is that, after a space discretization, the right hand side of the resulting ordinary differential equations has a very large Lipschitz constant caused by the Laplacian in the kinetic part. As a consequence, standard explicit integration schemes, such as the ones presented in [4], although very popular in computational physics, are of no use in quantum mechanical applications. Therefore, the treatment of such quantum dynamical systems has been of huge interest in the numerical analysis community for many decades, see, e.g., [3, Chapter II. 1]. Various evolution schemes for the linear Schrödinger equation in varying settings have been proposed over the years, see, e.g., [5, 6, 7, 8, 9, 10]. Nonlinear Schrödinger equations such as the Gross–Pitaevskii equation and equations arising from the Hartree and Hartree–Fock approximation of the quantum state have also been devoted attention to, see, e.g., [?, 13] and [14, 15], respectively.

All these methods have in common that the partial differential equations are first discretized in space. This means that the system is restricted to a suitable subspace spanned by a finite number of basis functions. Here, we do this with the help of a *Fourier collocation* method which is the straightforward approach for the problem we look at, see, e.g., [3, Chapter III. 1]. This yields a system of coupled ordinary differential equations, on the solution of which we focus in the present work.

[†]Mathematisches Institut, Universität Tübingen, Auf der Morgenstelle 10, D-72076 Tübingen, Germany. E-mail: seyrich@na.uni-tuebingen.de.

What, in many applications, turned out to be the most promising tool for the solution of the space discretized system was the splitting of the equations under consideration into some subproblems, each of which can be solved more easily than the system of equations as a whole. This idea was first employed for advection equations in [16] and [17]. In the realm of quantum dynamics, it was applied for the first time in [18] where the linear Hamiltonian was split into a kinetic and a potential part. The respective solutions were then concatenated in a suitable way in order to obtain a reliable integration method. Here, we use this ansatz to introduce two schemes for the evolution of the space discretized BCS equations. The CPU effort per time step of both these schemes depends only linearly on the number of basis functions. This is very important since in most physical applications the BCS system requires a discretization space of very high dimension.

For the first scheme, we exploit that the eigenvalues of the density operator, which are functions of the particle density and the Cooper pair density, are conserved along exact solutions to the BCS equations. Hence, we can express the particle density as a function of the Cooper pair density. We end up with a decoupled nonlinear system for the evolution of the Cooper pair density α . The thus obtained equations are split in a linear part, which can be solved exactly, and a nonlinear part, the flow of which can be approximated by some standard numerical scheme. In the rest of this work, we will refer to the resulting integrator as *BCSInt*. It is very accurate and preserves the physically interesting eigenvalues of the density operator by construction. The integrator has already been employed in a numerical study of the physical behavior of the BCS equations, see [19].

For the second integrator, we do not decouple the system at all. Instead, thanks to the system's particular structure, we can aptly split it into three subproblems for which the exact flows can be calculated very efficiently. These calculations require only basic operations. Recombining the thus obtained flows in a suitable way results in a very accurate and efficient scheme which conserves the system's constants of motion, such as the energy, up to very small errors. In the following, we will denote the new scheme by *SplitBCS*. We will demonstrate its advantages with the help of numerical experiments and numerical comparisons to the original scheme and to standard integration schemes. We mention that an error estimate similar to the one in [20] for splitting schemes applied to the Gross–Pitaevskii equations is expected to hold for *SplitBCS*. However, such an analysis is out of the scope of this work.

Our presentation is organized as follows: We start with a short introduction to the BCS equations in Section 1. Afterwards, we explain the Fourier collocation for the equations (0.1),(0.2) in Section 2. We first introduce our splitting scheme *BCSInt* for the decoupled nonlinear system in Section 3. Then, we present our fast integration scheme *SplitBCS* for the coupled system in Section 4. This is followed by numerical tests in Section 5. Finally, we summarize our results in Section 6.

1. The BCS equations. A superconducting translation invariant system in one spatial dimension is characterized by the particle density $\gamma : \mathbb{R} \times \mathbb{R} \mapsto \mathbb{R}$ which describes the probability at time t of finding a particle at position x and the Cooper pair density $\alpha : \mathbb{R} \times \mathbb{R} \mapsto \mathbb{C}$ which gives the probability at time t of having a Cooper pair of electrons at distance x . For a given particle interaction V , the evolution of α and γ is governed by the BCS equations, sometimes also called Bogolubov–De-Gennes

equations,

$$i\dot{\gamma}(t, x) = -2 \int_{\mathbb{R}} V(y) \operatorname{Im} [\alpha(t, x-y) \overline{\alpha(t, y)}] dy, \quad (1.1)$$

$$i\dot{\alpha}(t, x) = 2 \left(-\frac{d^2}{dx^2} - \mu + V(x) \right) \alpha(t, x) - 4 \int_{\mathbb{R}} \gamma(t, x-y) V(y) \alpha(t, y) dy, \quad (1.2)$$

with μ denoting the chemical potential of the physical system and $\dot{\cdot} = \partial/\partial t$. Conventionally, the BCS equations are given in terms of the Fourier transforms, i.e., the momentum space representations

$$\hat{\gamma}(t, p) = \frac{1}{2\pi} \int_{\mathbb{R}} \gamma(t, x) e^{ipx} dx, \quad (1.3)$$

$$\hat{\alpha}(t, p) = \frac{1}{2\pi} \int_{\mathbb{R}} \alpha(t, x) e^{ipx} dx. \quad (1.4)$$

In this basis, the equations can be written in the compact, self-consistent form

$$i\dot{\Gamma}(t, p) = [H_{\Gamma(t, p)}, \Gamma(t, p)], \quad p \in \mathbb{R}, \quad (1.5)$$

see, e.g., [21]. $\Gamma(t, p)$ is the 2×2 -matrix

$$\Gamma(t, p) = \begin{pmatrix} \hat{\gamma}(t, p) & \hat{\alpha}(t, p) \\ \hat{\alpha}(t, p) & 1 - \hat{\gamma}(t, p) \end{pmatrix} \quad (1.6)$$

and $H_{\Gamma(t, p)}$ is the Hamiltonian

$$H_{\Gamma(t, p)}(p) = \begin{pmatrix} p^2 - \mu & 2[\hat{V} * \hat{\alpha}](t, p) \\ 2[\hat{V} * \hat{\alpha}](t, p) & \mu - p^2 \end{pmatrix}. \quad (1.7)$$

Here, $*$ denotes the convolution of \hat{V} with $\hat{\alpha}(t, p)$.

1.1. Superconductivity. It can be shown, see e.g. [25], that the free energy functional

$$\mathcal{F}_T(\Gamma(t)) = \int_{\mathbb{R}} (p^2 - \mu) \hat{\gamma}(t, p) dp + \int_{\mathbb{R}} |\alpha(t, x)|^2 V(x) dx + \int_{\mathbb{R}} \operatorname{Tr}_{\mathbb{C}^2} (\Gamma(p) \log \Gamma(p)) dp \quad (1.8)$$

is conserved along solutions of the evolution equations (1.5) for any given temperature of the system T . If, for a given temperature T , the minimizer Γ of \mathcal{F}_T has a non vanishing Cooper pair density α , then the system is said to be in a superconducting state.

1.2. The discrete BCS equations. In order to render the system computationally palpable, one restricts it to a domain $D = [0, L2\pi]$, $L \in \mathbb{N}$, and assumes periodic boundary conditions. In most applications, L is a large integer as the extension of the system is considered to be huge compared to the microscopic scale which here is $\mathcal{O}(1)$. On the finite domain D , the momenta consist of the discrete set $k \in \frac{1}{L}\mathbb{Z}$. The momentum space representations of α and γ are given by

$$\hat{\gamma}_k(t) = \frac{1}{L2\pi} \int_0^{L2\pi} \gamma(t, x) e^{ikx} dx, \quad (1.9)$$

$$\hat{\alpha}_k(t) = \frac{1}{L2\pi} \int_0^{L2\pi} \alpha(t, x) e^{ikx} dx. \quad (1.10)$$

In terms of these representations, the BCS equations read

$$i\dot{\Gamma}_k(t) = [H_{\Gamma_k(t)}, \Gamma_k(t)], \quad k \in \frac{1}{L}\mathbb{Z}, \quad (1.11)$$

where the convolution appearing in the Hamiltonian is now to be understood as

$$\left(\hat{V} * \hat{\alpha}\right)_k(t) = \sum_{j \in \mathbb{Z}} \hat{V}_{k-j} \hat{\alpha}_j(t). \quad (1.12)$$

The first step to a numerical solution is to introduce a finite basis. This process is called *space discretization*.

2. Space discretization. As the BCS equations are given in their momentum space representation anyway, it is most convenient to use the so-called *Fourier collocation*. This means that for a fixed number $K \in \mathbb{N}$, a $L2\pi$ -periodic function $f(x) = \sum_{j \in \mathbb{Z}} \hat{f}(j) e^{ik/Lx}$ is approximated by

$$f^K(x) = \sum_{k=-\frac{K}{2}}^{\frac{K}{2}-1} \hat{f}_k^K e^{i\frac{k}{L}x}, \quad (2.1)$$

where the coefficients \hat{f}_k^K are obtained by the discrete Fourier transform of the values $f_j = f(L2\pi/K \cdot j)$, $j = -K/2, \dots, K/2-1$. From numerical analysis, cf. [3, Chapter III.1], it is known that for an s -times differentiable function f , the bound

$$\|f(x) - f^K(x)\| \leq CK^{-s} \left\| \frac{d^s f}{dx^s} \right\| \quad (2.2)$$

holds for some constant C independent of the number of basis functions K .

Mathematically speaking, we work on the subspace spanned by the first K eigenfunctions of the Laplacian on $[0, L2\pi]$ Laplacian. The approximation of the particle density on this subspace is given by

$$\gamma^K(t, x) = \sum_{k=-\frac{K}{2}}^{\frac{K}{2}-1} \hat{\gamma}_k^K(t) e^{i\frac{k}{L}x} \quad (2.3)$$

and the approximation of the Cooper pair density reads

$$\alpha^K(t, x) = \sum_{k=-\frac{K}{2}}^{\frac{K}{2}-1} \hat{\alpha}_k^K(t) e^{i\frac{k}{L}x}. \quad (2.4)$$

Inserting these approximations into the infinite dimensional BCS equations (1.11) yields a finite dimensional system of ordinary differential equations (ODEs).

2.1. System of ordinary differential equations. In order to derive this finite dimensional system, we first note that for a contact interaction $V(x) = -a\delta(x)$, $a > 0$, which is the most popular model for an interaction in physics, we have

$$\hat{V}(k) = -\frac{a}{2L\pi}, \quad -\frac{K}{2} \leq k \leq \frac{K}{2} - 1. \quad (2.5)$$

Hence, the convolution term in the self-consistent Hamiltonian on the K dimensional subspace is given by

$$\left(\hat{V} * \hat{\alpha}^K\right)_k(t) = -\frac{a}{2L\pi} \sum_{j=-\frac{K}{2}}^{\frac{K}{2}-1} \hat{\alpha}_j^K(t). \quad (2.6)$$

With this relation, a straightforward calculations of the matrix entries of the BCS equation (1.11) on the K dimensional subspace results in

$$i\dot{\gamma}_k(t) = -\frac{a}{L\pi} \left(\alpha_k(t) \sum_{j=-K/2}^{K/2-1} \alpha_j(t) - \overline{\alpha_k(t)} \sum_{j=-K/2}^{K/2-1} \alpha_j(t) \right), \quad (2.7)$$

$$i\dot{\alpha}_k(t) = 2 \left(\frac{k^2}{L^2} - \mu \right) \alpha_k(t) + \frac{a}{L\pi} \sum_{j=-K/2}^{K/2-1} \alpha_j(t) (2\gamma_k(t) - 1), \quad (2.8)$$

$$-\frac{K}{2} \leq k \leq \frac{K}{2} - 1,$$

where, for the sake of readability, we have replaced $\hat{\gamma}^K$ and $\hat{\alpha}^K$ by γ and α , respectively. With

$$p_k(t) := \operatorname{Re} \alpha_k(t), \quad (2.9)$$

$$q_k(t) := \operatorname{Im} \alpha_k(t), \quad (2.10)$$

we can rewrite the equation of motion for $\gamma_k(t)$ as

$$\dot{\gamma}_k(t) = \frac{2a}{L\pi} \left(q_k(t) \sum_{j=-K/2}^{K/2-1} p_j(t) - p_k(t) \sum_{j=-K/2}^{K/2-1} q_j(t) \right). \quad (2.11)$$

This shows that $\gamma_k(t)$ is a real quantity whenever $\gamma_t(0)$ is so. As γ represents the physical particle density which is real by definition, we can safely assume $\gamma_k(t)$ to be real in the following.

2.2. Constants of motion. For later use we mention that the coupled system (2.11),(2.8) possesses some important constants of motion:

- It can readily be seen that the matrix $H_{\Gamma(t)}$ in the BCS equations (1.11) is self-adjoint. Together with the commutator structure of the equations of motion (1.11), this implies that the evolution of $\Gamma(t)$ is unitary. Consequently, its eigenvalues are preserved along the evolution. A little bit of algebra shows that these eigenvalues are given by

$$\lambda_k^\pm = \frac{1}{2} \pm \sqrt{\left(\gamma_k(t) - \frac{1}{2}\right)^2 + |\alpha_k(t)|^2}. \quad (2.12)$$

- The discretized analog of the free energy functional (1.8) in the case of an interaction potential is given by

$$\begin{aligned} F^K(\gamma(t), \alpha(t)) &:= \sum_{k=-K/2}^{K/2-1} \left(\frac{k^2}{L^2} - \mu \right) \gamma_k(t) - \frac{a}{L2\pi} \left(\sum_{k=-K/2}^{K/2-1} |p_k(t)|^2 + |q_k(t)|^2 \right), \\ &+ T \sum_{k=-K/2}^{K/2-1} [\lambda_k^+ \log(\lambda_k^+) + \lambda_k^- \log(\lambda_k^-)], \end{aligned} \quad (2.13)$$

and can be shown to be preserved, too.

2.3. Numerical notation. From a numerical point of view, the coupled system (2.11),(2.8), when supplemented by some initial data, represents an initial value problem

$$\begin{cases} \frac{d\mathbf{y}(t)}{dt} &= f(\mathbf{y}(t)), \\ \mathbf{y}(0) &= \mathbf{y}_0, \end{cases} \quad (2.14)$$

with $\mathbf{y} \in \mathbb{C}^{2K}$. Formally, the aim of this paper is to find a numerical approximation to the exact flow of such an initial value problem. For this, we denote a time step by τ and the flow over such a time, i.e., the smooth map between $\mathbf{y}(t)$ and $\mathbf{y}(t + \tau)$, by $\Phi_{\tau,f}(\mathbf{y}(t))$. Its numerical approximation will be denoted by $\Phi_{\tau,f}^{\text{num}}$.

Let us now turn towards our first algorithm for the calculation of this numerical flow.

3. Nonlinear splitting integrator. BCSInt, the integrator we present in this Section, is based on the conservation of the eigenvalues of $\Gamma(t)$. These eigenvalues being conserved, the following equality holds

$$\left(\gamma_k(t) - \frac{1}{2}\right)^2 + |\alpha_k(t)|^2 = \left(\gamma_k(0) - \frac{1}{2}\right)^2 + |\alpha_k(0)|^2. \quad (3.1)$$

With the help of this relation, we can eliminate $\gamma_k(t)$ in the equations of motion for $\alpha_k(t)$ as we show now.

3.1. Decoupled system. Solving Eq. (3.1) for γ_k yields

$$\gamma_k(t) = \frac{1}{2} \pm \sqrt{h(k) - |\alpha_k(t)|^2}, \quad (3.2)$$

with the auxiliary function

$$h(k) := \left(\gamma_k(0) - \frac{1}{2}\right)^2 + |\alpha_k(0)|^2. \quad (3.3)$$

The sign in relation (3.2) can usually be inferred from physical information. For example, in our study [19], the initial values had to be such that $\gamma_k(0)$ was greater than $1/2$ for $\mu > k^2/L^2$ and less than or equal to $1/2$ for $\mu \leq k^2/L^2$.

Inserting the just-derived expression (3.2) for $\gamma_k(t)$ into the equations of motion for $\alpha_k(t)$, we get the nonlinear system

$$\begin{aligned} i\dot{\alpha}_k(t) &= 2 \left(\frac{k^2}{L^2} - \mu \right) \alpha_k(t) \pm \frac{a}{L\pi} \sqrt{h(k) - |\alpha_k(t)|^2} \sum_{j=-K/2}^{K/2-1} \alpha_t(j), \\ -\frac{K}{2} &\leq k \leq \frac{K}{2} - 1. \end{aligned} \quad (3.4)$$

Having decoupled the system, we can now turn towards its time evolution.

3.2. BCSInt. The nonlinear system (3.4), together with some suitable initial data, gives an initial value problem

$$\begin{cases} \frac{d\vec{\alpha}(t)}{dt} &= \tilde{f}(\vec{\alpha}(t)), \\ \vec{\alpha}(0) &= \vec{\alpha}_0, \end{cases} \quad (3.5)$$

for

$$\vec{\alpha} = (\alpha_{-\kappa/2}(t) \quad \dots \quad \alpha_{\kappa/2-1}(t))^T \in \mathbb{C}^K. \quad (3.6)$$

The right hand side of the differential equation can be written as the sum of two terms,

$$\tilde{f}(\vec{\alpha}) = A\vec{\alpha} + f_1(\vec{\alpha}), \quad (3.7)$$

where f_1 represents the nonlinear term and where A is the matrix

$$A = \text{diag} \left(2 \left(\frac{(-\frac{K}{2})^2}{L^2} - \mu \right), \dots, 2 \left(\frac{(\frac{K}{2}-1)^2}{L^2} - \mu \right) \right). \quad (3.8)$$

This linear part resembles the kinetic part of the linear Schrödinger equation. Its flow $\Phi_{\tau,A}$ can be calculated exactly as

$$\Phi_{\tau,A}(\vec{\alpha}) = e^{-i2\left(\frac{K^2}{L^2} - \mu\right)\tau} \vec{\alpha}. \quad (3.9)$$

With regard to f_1 , it has a much smaller Lipschitz constant than the complete right hand side f , wherefore Φ_{τ,f_1} can be approximated by some standard integration scheme. We then follow the idea of [16] and set

$$\Phi_{\tau,\tilde{f}}^{\text{num}}(\vec{\alpha}(0)) = (\Phi_{\tau/2,A} \circ \Phi_{\tau,f_1}^{\text{num}} \circ \Phi_{\tau/2,A})(\vec{\alpha}(0)). \quad (3.10)$$

Applying this operation successively yields an approximation to the exact solution at times $t = n\tau$, $n = 1, 2, \dots$. Its error decreases quadratically as a function of the step size τ as long as $\Phi_{\tau,f_1}^{\text{num}}$ is a second-or-higher order approximation to Φ_{τ,f_1} , see, e.g. [22, Chapter II.5].

Just as every exact flow, $\Phi_{\tau,A}$ satisfies

$$\Phi_{t,A} \circ \Phi_{s,A} = \Phi_{t+s,A}. \quad (3.11)$$

Hence, when applying many time steps of the numerical scheme in a row, one can combine the last sub-step of the previous step with the first sub-step of the next step, thus saving computational costs. We illustrate the resulting procedure in Fig. 3.1.

Algorithm 1: BCSInt

```

 $\vec{\alpha} = \Phi_{\tau/2,A}(\vec{\alpha}_0)$ 
for  $n = 0$  to  $N$  do
     $\vec{\alpha} = \Phi_{\tau,f_1}^{\text{num}}(\vec{\alpha}).$ 
     $\vec{\alpha} = \Phi_{\tau,A}(\vec{\alpha}).$ 
 $\vec{\alpha} = \Phi_{-\tau/2,A}(\vec{\alpha})$ 

```

Figure 3.1: Sketch of our algorithm BCSInt which for a given initial value $\vec{\alpha}_0$ and a given step size τ approximates $\vec{\alpha}(N\tau) = \Phi_{N\tau,\tilde{f}}(\vec{\alpha}_0)$.

Concerning $\Phi_{\tau,f_1}^{\text{num}}$, in the study [19] it has been calculated via the fifth order explicit Cash–Karp Runge–Kutta scheme proposed in [4]. In the experiment Section 5 below, we will also test the second order explicit midpoint rule. In this case, $\Phi_{\tau,f_1}^{\text{num}}$ is calculated as outlined in Fig. 3.2.

Algorithm 2: $\text{calc}\Phi_{f_1}$	Algorithm 3: $\text{calc}f_1$
$\dot{\mathbf{Y}} = \text{calc}f_1(\vec{\alpha})$ for $k = -K/2$ to $K/2 - 1$ do $Y(k) = \alpha_k(t) + \tau/2 \dot{\mathbf{Y}}(k)$ $\dot{\mathbf{Y}} = \text{calc}f_1(\mathbf{Y})$ for $k = -K/2$ to $K/2 - 1$ do $\alpha_k(t) = \alpha_k(t) + \tau \dot{\mathbf{Y}}(k)$	$s = a/(L\pi) \cdot \sum_{k=-K/2}^{K/2-1} \alpha_k(t)$ for $k = -K/2$ to $K/2 - 1$ do $c = \sqrt{h(k) - \alpha_k(t) ^2}$ $f_1(k) = c \cdot s$

Figure 3.2: The left panel shows the algorithm which for a given value $\vec{\alpha}(n\tau)$ and a given time step τ calculates $\vec{\alpha}((n+1)\tau) = \Phi_{\tau, f_1}^{\text{num}}(\vec{\alpha}(n\tau))$ with the explicit midpoint rule. The right panel shows the algorithm which for a given value $\vec{\alpha}$ calculates $f_1(\vec{\alpha})$.

3.3. Number of operations. In order to analyze BCSInt's efficiency, we count the number of real operations which are executed per call of our implementations, which, to the best of our knowledge, have been implemented in the most efficient way possible. We do not weight the costs of different operations, i.e., the square root in $\text{calc}f_1$, cf. Fig. 3.2, also counts as a single operation. The number of operations as a function of the number of basis functions K for the various sub-algorithms and BCSInt as a whole are listed in Tab. 3.1. We mention that, if we substituted the fifth order Cash–Karp scheme for the explicit midpoint rule in $\text{calc}\Phi_{f_1}$, the number of operations for $\text{calc}\Phi_{f_1}$ would increase to $184 \cdot K$.

Algorithm	#Operations per call
Calculation of $\Phi_{\tau, A}$	$14 \cdot K + 14$
$\text{Calc}f_1$	$18 \cdot K + 20$
$\text{calc}\Phi_{f_1}$	$2 \times \text{calc}f_1 + 8 \cdot K + 9 = 44 \cdot K + 49$
BCSInt	$58 \cdot K + 63$

Table 3.1: The required number of operations per step as a function of the dimension of the ODE system (3.4) for the sub-algorithms of BCSInt and for BCSInt itself.

Let us now introduce our second, more efficient and yet more accurate integration scheme.

4. Fast splitting integrator. For our second scheme, we consider the coupled system (2.7),(2.8) as a whole. From a numerical perspective, we have an initial value problem for

$$\mathbf{y}(t) = \begin{pmatrix} \vec{\gamma}(t) \\ \vec{\alpha}(t) \end{pmatrix} \in \mathbb{C}^{2K}, \quad (4.1)$$

$$\vec{\gamma}(t) = (\gamma_{-K/2}(t) \quad \dots \quad \gamma_{K/2-1}(t))^T \in \mathbb{R}^K, \quad (4.2)$$

$$\vec{\alpha}(t) = (\alpha_{-K/2}(t) \quad \dots \quad \alpha_{K/2-1}(t))^T \in \mathbb{C}^K, \quad (4.3)$$

$$(4.4)$$

whose right hand side $f(\mathbf{y})$ can be split into three parts,

$$f(\vec{\gamma}, \vec{\alpha}) = \tilde{A}\mathbf{y} + g(\vec{\alpha}) + h(\vec{\gamma}, \vec{\alpha}). \quad (4.5)$$

Here, $\tilde{A}\mathbf{y}$ is the first term of the equation of motion (2.8) for α , i.e.,

$$\tilde{A} \begin{pmatrix} \vec{\gamma} \\ \vec{\alpha} \end{pmatrix} = \begin{pmatrix} \vec{\gamma} \\ A\vec{\alpha} \end{pmatrix}, \quad (4.6)$$

which means that it represents the same action on α as A in the nonlinear case above. The function $g(\vec{\alpha})$ represents the right hand side of the evolution equation for γ and $h(\vec{\gamma}, \vec{\alpha})$ is the second term of Eq. (2.8).

We will now show that we can efficiently calculate the exact flows for all three subproblems. The calculation of $\Phi_{\tau, \tilde{A}}$ is nothing other than $\Phi_{\tau, A}$ acting on $\vec{\alpha}$ with $\vec{\gamma}$ held constant. We thus, in fact, only have to consider the other two subproblems.

4.1. Calculating $\Phi_{\tau, g}$. For the subsystem

$$\begin{cases} \frac{d\vec{\gamma}(t)}{dt} &= g(\vec{\alpha}(t)), \\ \vec{\gamma}(0) &= \vec{\gamma}_0, \end{cases} \quad (4.7)$$

the right hand side does not depend on the quantity to be evolved. Therefore, the solution of the initial value problem (4.7) at time t is trivially given by

$$\vec{\gamma}(t) = \Phi_{t, g}(\vec{\gamma}(0)) = \vec{\gamma}(0) + t \cdot g(\vec{\alpha}(0)). \quad (4.8)$$

Bearing in mind the reformulation (2.11), we calculate a step of $\Phi_{\tau, g}$ with the algorithm illustrated in Fig. 4.1.

Algorithm 4: calc Φ_g

```

 $p = 2a/(L\pi) \sum_{k=-\frac{K}{2}}^{\frac{K}{2}-1} p_k$ 
 $q = 2a/(L\pi) \sum_{k=-\frac{K}{2}}^{\frac{K}{2}-1} q_k$ 
for  $k = -K/2$  to  $K/2 - 1$  do
   $\gamma_k(t) = \gamma_k(0) + \tau \cdot (q_k \cdot p - p_k \cdot q)$ 

```

Figure 4.1: Sketch of the algorithm which for given values $\vec{\gamma}(0)$, $\vec{\alpha}(0)$ and a given step size τ calculates the solution $\vec{\gamma}(\tau) = \Phi_{\tau, g}(\vec{\gamma}(0))$ to the initial value problem (4.7).

4.2. Calculating $\Phi_{\tau, h}$. We consider the subproblem

$$\begin{cases} \frac{d\vec{\alpha}(t)}{dt} &= h(\vec{\gamma}(0), \vec{\alpha}(t)), \\ \vec{\alpha}(0) &= \vec{\alpha}_0. \end{cases} \quad (4.9)$$

Introducing $\vec{b} \in \mathbb{R}^K$ via

$$b_k = \frac{a}{L\pi} (2\gamma_k(0) - 1) \quad (4.10)$$

and the $K \times K$ -matrix

$$B = \underbrace{\begin{pmatrix} b_{-K/2} & \dots & b_{-K/2} \\ \vdots & \ddots & \vdots \\ b_{K/2-1} & \dots & b_{K/2-1} \end{pmatrix}}_K, \quad (4.11)$$

we can write

$$h(\vec{\gamma}(0), \vec{\alpha}(t)) = B\vec{\alpha}(t). \quad (4.12)$$

Hence, the solution to the initial value problem (4.9) is given by

$$\vec{\alpha}(\tau) = \Phi_{\tau,h}(\vec{\alpha}(0)) = e^{-iB\tau}\vec{\alpha}(0) =: e^{\tilde{B}}\vec{\alpha}(0). \quad (4.13)$$

We now show that for a given $\vec{\alpha}(0)$, $\vec{\alpha}(\tau)$ can be calculated in $\mathcal{O}(K)$ operations.

For a given $n \in \mathbb{N}$, we have

$$\tilde{B}^n = \underbrace{\begin{pmatrix} -ib_{-K/2}\tau c^{n-1} & \dots & -ib_{-K/2}\tau c^{n-1} \\ \vdots & \ddots & \vdots \\ -ib_{K/2-1}\tau c^{n-1} & \dots & -ib_{K/2-1}\tau c^{n-1} \end{pmatrix}}_K, \quad (4.14)$$

with

$$c = -i\tau \sum_{j=-\frac{K}{2}}^{\frac{K}{2}-1} b_j, \quad (4.15)$$

Consequently, with Id denoting the $K \times K$ identity matrix, we have

$$\exp(-i\tau B) = \text{Id} + \sum_{n=1}^{\infty} \frac{1}{n!} \begin{pmatrix} -ib_{-K/2}\tau c^{n-1} & \dots & -ib_{-K/2}\tau c^{n-1} \\ \vdots & \ddots & \vdots \\ -ib_{K/2-1}\tau c^{n-1} & \dots & -ib_{K/2-1}\tau c^{n-1} \end{pmatrix} \quad (4.16)$$

$$= \text{Id} + \frac{1}{c} \begin{pmatrix} -ib_{-K/2}\tau(\exp(c) - 1) & \dots & -ib_{-K/2}\tau(\exp(c) - 1) \\ \vdots & \ddots & \vdots \\ -ib_{K/2-1}\tau(\exp(c) - 1) & \dots & -ib_{K/2-1}\tau(\exp(c) - 1) \end{pmatrix}. \quad (4.17)$$

With this, the matrix-vector multiplication in Eq. (4.13) yields

$$\exp(-i\tau B)\vec{\alpha}(0) = \vec{\alpha}(0) - \frac{i\tau}{c} \begin{pmatrix} b_{-K/2}(\exp(c) - 1) \sum_{j=-\frac{K}{2}}^{\frac{K}{2}-1} \alpha_j(0) \\ \vdots \\ b_{K/2-1}(\exp(c) - 1) \sum_{j=-\frac{K}{2}}^{\frac{K}{2}-1} \alpha_j(0) \end{pmatrix}. \quad (4.18)$$

Thus, the solution of the initial value problem (4.9) can efficiently be calculated by the algorithm illustrated in Fig. 4.2.

Having found efficient algorithms for all three subproblems we have split the system into, we can now recompose them.

Algorithm 5: calc Φ_h

```

 $c = -i\tau \sum_{k=-\frac{K}{2}}^{\frac{K}{2}-1} b_k$ 
 $s = \sum_{k=-\frac{K}{2}}^{\frac{K}{2}-1} \alpha_k(0)$ 
 $e = \exp(c) - 1$ 
for  $k = -K/2$  to  $K/2 - 1$  do
     $\alpha_k(t) = \alpha_k(0) - i\tau \cdot e \cdot s \cdot b_k/c$ 

```

Figure 4.2: Sketch of the algorithm which for given values $\vec{\gamma}(0)$, $\vec{\alpha}(0)$ and a given step size τ calculates the solution $\vec{\alpha}(\tau) = \Phi_{\tau,h}(\vec{\alpha}(0))$ to the initial value problem (4.9).

4.3. SplitBCS. As all the three flows $\Phi_{\tau,A}$, $\Phi_{\tau,g}$, and $\Phi_{\tau,h}$ are given exactly, each symmetric composition of them gives rise to a second order integration scheme, see, e.g. [22, Chapter II.5]. We propose the composition

$$\Phi_{\tau,f}^{\text{num}} = \Phi_{\tau,AghgA} := \Phi_{\tau/2,A} \circ \Phi_{\tau/2,g} \circ \Phi_{\tau,h} \circ \Phi_{\tau/2,g} \circ \Phi_{\tau/2,A}, \quad (4.19)$$

as this yields the fastest and most accurate scheme among the possible combinations as we will see in the next Section. If even more accuracy were required, we could use a suitable composition of the scheme (4.19); see [23, 24] for more information on compositions.

In the same way as for the algorithm of Section 3, the last sub-step of each step can be combined with the first sub-step of the following step which reduces the CPU effort. Even more computational costs can be saved by paying heed to the following points.

- From Eq. (2.11) it can be deduced that

$$\frac{d}{dt} \left(\sum_{j=-\frac{K}{2}}^{\frac{K}{2}-1} \gamma_k(t) \right) = 0. \quad (4.20)$$

Thus, the sum over all $\gamma_k(t)$, and, as a consequence, also the quantities c and e appearing in the calculation of $\Phi_{\tau,h}$, cf. Fig. 4.2, are preserved along evolutions of the equations of motion. Hence, c and e only need to be calculated once at the start of the simulation.

- Both $\Phi_{\tau,g}$ and $\Phi_{\tau,h}$ require the calculation of the sum over all $\alpha_k(t)$, cf. Figs. 4.1 and 4.2. However, $\Phi_{\tau,g}$ does not modify $\vec{\alpha}$, which means that the sum over all $\alpha_k(t)$ in calc Φ_h is the same as the one already calculated in calc Φ_g . Hence, by suitably combining the calculation of

$$\Phi_{\tau,ghg} := \Phi_{\tau/2,g} \circ \Phi_{\tau,h} \circ \Phi_{\tau/2,g} \quad (4.21)$$

into one algorithm, one can avoid redundancies¹.

- The calculation of $\Phi_{\tau,A}$ can be made more efficient for both BCSInt and SplitBCS when a fixed step size is used. In this case, during each call of $\Phi_{\tau,A}$, \cos and \sin of $2 \left(k^2/L^2 - \mu \right) \tau$, $k = K/2, \dots, K/2 - 1$, have to be calculated.

¹An efficient implementation of $\Phi_{\tau,ghg}$ in c++ can be found on the author's homepage <http://na.uni-tuebingen.de/~seyrich/>.

However, if storage is not a problem, one only has to calculate the cos and sin once at the beginning of the simulation as the arguments are the same in each step. This is what we did in our implementations. Accordingly, the number of operations specified in Tabs. 3.1 and 4.1, refer to this efficient version.

Putting everything together, we obtain our integrator SplitBCS as outlined in Fig. 4.3.

Algorithm 6: SplitBCS

```

 $\vec{\alpha} = \Phi_{\tau/2,A}(\vec{\alpha}(0))$ 
for  $n = 0$  to  $N$  do
     $(\vec{\gamma}, \vec{\alpha}) = \Phi_{\tau,ghg}(\vec{\gamma}, \vec{\alpha}).$ 
     $\vec{\alpha} = \Phi_{\tau,A}(\vec{\alpha}).$ 
 $\vec{\alpha} = \Phi_{-\tau/2,A}(\vec{\alpha})$ 

```

Figure 4.3: Sketch of our algorithm SplitBCS which for given initial values $\vec{\gamma}(0)$, $\vec{\alpha}(0)$ and a given step size τ approximates $(\vec{\gamma}(N\tau), \vec{\alpha}(N\tau))^T = \Phi_{N\tau,f}(\vec{\gamma}(0), \vec{\alpha}(0))$.

4.4. Number of operations. In order to compare the efficiency of SplitBCS to the one of BCSInt, we here, too, count the number of operations required for the respective sub-algorithms and for SplitBCS as a whole. The result can be found in Tab. 4.1. We see that SplitBCS requires roughly half as many operations as BCSInt.

Algorithm	#Operations per call
Calculation of $\Phi_{\tau,A}$	$14 \cdot K + 14$
calc Φ_h	$11 \cdot K + 23$
calc Φ_g	$11 \cdot K + 17$
Calculation of $\Phi_{\tau,ghg}$	$18 \cdot K + 39$
SplitBCS	$32 \cdot K + 53$

Table 4.1: The required number of operations per step as a function of dimension of the ODE system (2.7),(2.8) for the sub-algorithms of SplitBCS and for SplitBCS itself.

Very importantly, SplitBCS only relies on the basic operations $=, -, \cdot, /$ acting on arrays. No nontrivial function, such as the square root in $\text{calc}\Phi_{f_1}$ of BCSInt, is required. We further see that suitably combining the calculations of the flows of $\Phi_{\tau,g}$, $\Phi_{\tau,h}$ in one algorithm reduces the number of operations from $\mathcal{O}(33 \cdot K)$ to $\mathcal{O}(18 \cdot K)$. This is why we choose the composition (4.19) over other possible sequences of the sub-flows.

Let us now subject the schemes to numerical tests.

5. Numerical experiments. All the numerical experiments presented here were run on a Core 2 Duo E6600 machine with 2.4GHz and 4GB RAM. In order to have physically realistic data to start our experiments with, we choose a system

which is slightly superconducting. Such a system can be obtained by setting

$$\hat{\gamma}_k(0) = \frac{1}{2} - \frac{k^2/L^2 - \mu}{2} \frac{\tanh\left(\frac{\sqrt{(k^2/L^2 - \mu)^2 + h^2}}{2T}\right)}{\sqrt{(k^2/L^2 - \mu)^2 + h^2}} \quad (5.1)$$

$$\hat{\alpha}_k(0) = \frac{h}{2} \frac{\tanh\left(\frac{\sqrt{(k^2/L^2 - \mu)^2 + h^2}}{2T}\right)}{\sqrt{(k^2/L^2 - \mu)^2 + h^2}}, \quad (5.2)$$

where $h = 0.1$ is a small parameter. The critical temperature T of the system depends on the interaction strength a and the chemical potential μ . It can be calculated from the implicit formula

$$\frac{2\pi}{a} = \int_{\mathbb{R}} \frac{\tanh\left(\frac{p^2 - \mu}{2T}\right)}{p^2 - \mu} dp. \quad (5.3)$$

For our simulations, we choose $a = \mu = 1$ which yields $T = 0.19$.

With reasonable initial data now at hand, we first want to corroborate our reasoning in Subsections 3.3 and 4.4 concerning the efficiency of the schemes.

5.1. Testing the efficiency. In order to test the algorithms and sub-algorithms of Sections 3 and 4 for their required CPU times, we fixed $L = 32$ and $K = 128 \cdot L$, chose a very small step size of $\tau = 10^{-6}$, and ran every sub-algorithm which is part of BCSInt or SplitBCS for 10^6 successive times. The resulting CPU times are listed in Tab. 5.1. We clearly see that the calculation of $\Phi_{\tau,ghg}$ is much faster than the

Algorithm	CPU times
Calculation of $\Phi_{\tau,A}$ with calculation of sin and cos	293.6
Calculation of $\Phi_{\tau,A}$	182.3
Calc f_1	58.0
calc Φ_{f_1} with explicit midpoint rule	158.2
calc Φ_{f_1} with Cash–Karp	714.1
calc Φ_h	33.2
calc Φ_g	29.3
Calculation of $\Phi_{\tau,ghg}$	71.3

Table 5.1: The CPU times in [s] for 10^6 successive runs of the various sub-algorithms making up BCSInt and SplitBCS.

calculation of the flow of the nonlinear part Φ_{τ,f_1} . A repetition of the procedure for $L = 64$ showed the same differences between the respective CPU times.

Thus, SplitBCS is much more efficient than BCSInt. Let us next compare the schemes' accuracies.

5.2. Testing the accuracy. As a measure of an integrator's accuracy, we consider the discrete energy (2.13) which is conserved along the exact solution of the ODE system (2.7),(2.8). Thus, the reliability of a numerical integration scheme can be checked by tracking the relative error ΔF^K , defined by

$$\Delta F^K(t) = \left| \frac{F^K(\vec{\gamma}(t), \vec{\alpha}(t)) - F^K(\vec{\gamma}(0), \vec{\alpha}(0))}{F^K(\vec{\gamma}(0), \vec{\alpha}(0))} \right|, \quad (5.4)$$

along the numerical evolution.

We first used this tool to compare SplitBCS to BCSInt with Φ_{τ, f_1} calculated via the fifth order Cash–Karp method. For this, we fixed $L = 32$, $K = 256 \cdot L$ and chose a step size $\tau = 0.1/K$. We evolved the system until $t = \mathcal{O}(L)$ with both integrators and plotted the relative error in the energy, ΔF^K , against integration time t in the left panel of Fig. 5.1. We repeated the procedure for $L = 64$ and plotted the result in the right panel of Fig. 5.1. For both cases the error grows at the end of the simulation

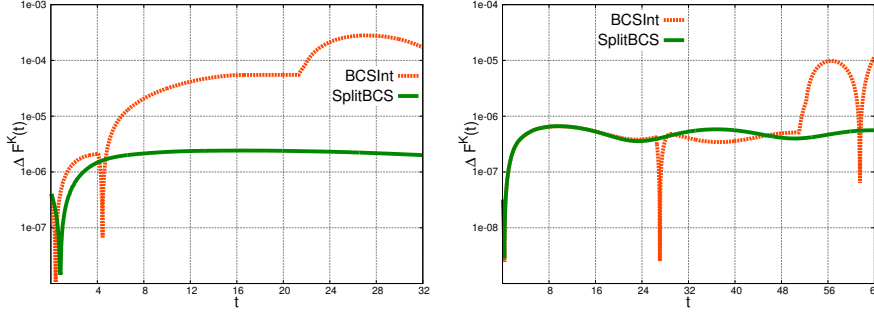


Figure 5.1: The relative error ΔF^K of the free energy as a function of integration time t for SplitBCS and BCSInt in semilogarithmic scale. The left panel shows the result for $L = 32$, the right panel depicts the corresponding result for $L = 64$.

when using BCSInt but not so for SplitBCS.

One could object that the reduced overall accuracy of BCSInt is offset by its exact preservation of the eigenvalues λ_k of the particle density matrix Γ . However, during the aforementioned simulations we also tracked the relative errors of the eigenvalues

$$\Delta \lambda_k(t) = \left| \frac{\lambda_k(t) - \lambda_k(0)}{\lambda_k(0)} \right|, \quad (5.5)$$

for SplitBCS. We found out that, up to very small rounding errors, all eigenvalues were preserved for SplitBCS, too. As an illustration, we plot the corresponding relative error for λ_0 in Fig. 5.2.

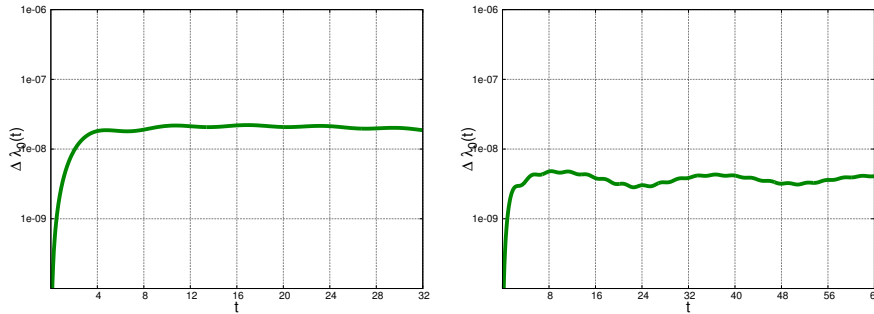


Figure 5.2: The relative error $\Delta \lambda_0$ of density matrix' first eigenvalue as a function of integration time t for SplitBCS in semilogarithmic scale. The left panel shows the result for $L = 32$, the right panel depicts the corresponding result for $L = 64$.

Still, the question remains as to whether we could have done even better by choosing another sequence of the sub-flows than composition (4.19). In order to go into this matter, we also evolved the systems for $L = 32$ and $L = 64$ for various other compositions of the sub-flows $\Phi_{\tau,A}$, $\Phi_{\tau,g}$ and $\Phi_{\tau,h}$, and again plotted ΔF^K as a function of the integration time t . The resulting plots are shown in Fig. 5.3. We also

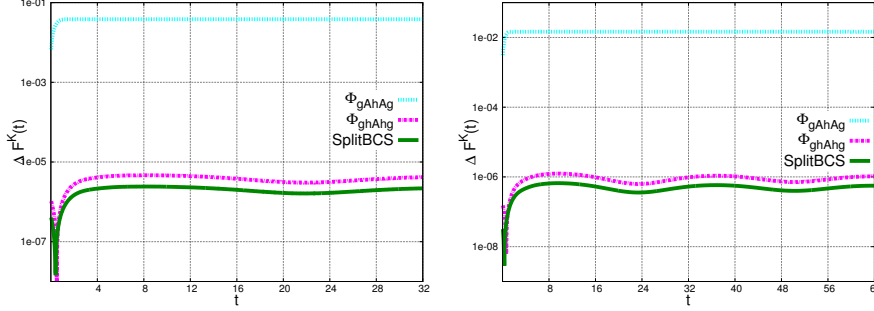


Figure 5.3: The relative error ΔF^K of the free energy as a function of integration time t for SplitBCS and other possible compositions in semilogarithmic scale. The left panel shows the result for $L = 32$, the right panel depicts the corresponding result for $L = 64$.

tested the other possible sequences which are not shown in the plots. However, we found out that the relative error in the energy seems only to depend on the position of $\Phi_{\tau,A}$ in the composition. This means that $\Phi_{\tau,AhghA}$ is as accurate as SplitBCS. But we could not find an equally efficient implementation for $\Phi_{\tau,hgh}$ as the one for $\Phi_{\tau,ghg}$. This is why we strongly recommend the use of the composition (4.19), shortly SplitBCS, in simulations of the discrete BCS equations.

In order to show, as a last point, why standard integration schemes are of no use for the discrete BCS equations, we apply the popular fifth order Cash–Karp scheme of [4] to the equations with the same L and the same step size as for the splitting methods. When plotting the resulting ΔF^K , cf. Fig 5.4, we observe an exponential growth in the error. This is in accordance with theoretical expectations, see, e.g. [26].

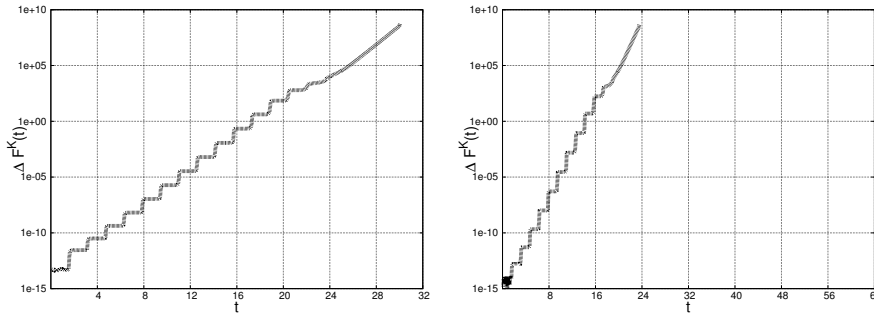


Figure 5.4: The relative error ΔF^K of the free energy as a function of integration time t for the explicit Cash–Karp scheme in semilogarithmic scale. The left panel shows the result for $L = 32$, the right panel depicts the corresponding result for $L = 64$.

Let us now summarize our results.

6. Conclusion. In this work, we have presented a fast and accurate evolution scheme, SplitBCS, for the coupled, discrete BCS equations which arise from a Fourier space discretization of the BCS equations for superconducting materials. SplitBCS is based on a splitting of the coupled equations into subproblems which can all be solved exactly by employing basic operations only. Crucially, the CPU effort for these exact solutions grows only linearly in the dimension of the spatial discretization. Further computational costs could be saved by aptly recombining the flows of the subproblems. In numerical tests, SplitBCS has been shown to be faster and more accurate than either standard integration schemes or a nonlinear splitting scheme. Additionally, it preserves the discrete analog of the physical energy and the eigenvalues of the particle density matrix up to very small errors. We have, thus, come up with a very useful tool for simulations in the field of superconductivity.

Acknowledgements: I would like to thank Ch. Hainzl and Ch. Lubich for useful discussions and suggestions. This work was partially funded by the DFG grant GRK 1838.

REFERENCES

- [1] J. BARDEEN, L. N. COOPER AND J. R. SCHRIEFER, *Theory of superconductivity*, Physical Review, 108 (1957), pp. 1175-1204.
- [2] V. BACH, E. H. LIEB AND J. P. SOLOVEJ, *Generalized Hartree-Fock theory and the Hubbard model*, Journal of statistical physics, 76 (1994), pp. 3-89.
- [3] CH. LUBICH, *From Quantum to Classical Molecular Dynamics: Reduced Models and Numerical Analysis*, Europ. Math. Soc., Zurich, 2008.
- [4] W. PRESS, S. TEUKOLSKY, W. VETTERLING AND B. FLANNERY, *Numerical Recipes in C. The art of scientific computing*, Cambridge University Press, Cambridge, 1992, 2nd edition.
- [5] S. K. GRAY AND D. E. MANOLOPOULOS, *Symplectic integrators tailored to the time-dependent Schrödinger equation*, J. Comput. Phys., 104(1996), pp. 7099-7112.
- [6] S. BLANES, F. CASAS AND A. MURUA, *Symplectic splitting operator methods for the time-dependent Schrödinger equation*, J. Comput. Phys., 124(2006), pp. 234105.
- [7] H. TAL-EZER AND R. KOSLOFF, *An accurate and efficient scheme for propagating the time dependent Schrödinger equation*, J. Chem. Phys., 81(1984), pp. 3967-3971.
- [8] T. J. PARK AND J. C. LIGHT, *Unitary quantum time evolution by iterative Lanczos reduction*, J. Chem. Phys., 85(1986), pp. 5870-5876.
- [9] M. HOCHBRUCK AND CH. LUBICH, *On Krylov subspace approximations to the matrix exponential operator*, SIAM J. Num. Anal., 34 (1997), pp. 1911-1925.
- [10] M. HOCHBRUCK AND CH. LUBICH, *On Magnus integrators for time-dependent Schrödinger equations*, SIAM J. Num. Anal., 41 (2003), pp. 945-963.
- [11] Y.-F. TANG, L. VÁZQUEZ, F. ZHANG AND V. M. PÉREZ-GARCÍA, *Symplectic methods for the nonlinear Schrödinger equation*, Computers Math. Applic., 32 (1996), pp. 73-83.
- [12] W. BAO, D. JAKSCH AND P. A. MARKOWICH, *Numerical solution of the Gross-Pitaevskii equation for Bose-Einstein condensation*, J. Comput. Phys., 187 (2003), pp. 318-342.
- [13] L. GAUCKLER AND CH. LUBICH, *Splitting integrators for nonlinear Schrödinger equations over long times*, Found. Comput. Math., 10 (2010), pp. 275-302.
- [14] CH. LUBICH, *A variational splitting integrator for quantum molecular dynamics*, Appl. Numer. Math., 48 (2004), pp. 355-368.
- [15] CH. LUBICH, *On variational approximations in quantum molecular dynamics*, Math. Comp., 74 (2005), pp. 765-779.
- [16] G. STRANG, *On the construction and comparison of difference schemes*, SIAM J. Numer. Anal., 5 (1968), pp. 506-517.
- [17] G. MARCHUCK, *Some applications of splitting-up methods to the solution of mathematical physics problems*, Aplikace Matematiky, 13 (1968), pp. 103-132.
- [18] M. D. FEIT, J. A. FLECK JR. AND A. STEIGER, *Solution of the Schrödinger equation by a spectral method*, Math. Comp., 47 (1982), pp. 412-433.
- [19] CH. HAINZL AND J. SEYRICH, *Comparing the full time-dependent BCS equation to its linear approximation: A numerical investigation*, arXiv preprint arXiv:1504.05881 (2015).

- [20] L. GAUCKLER, *Convergence of a split-step Hermite method for the Gross-Pitaevskii equation*, IMA Journal of Numerical Analysis, 31 (2011), pp. 396-415.
- [21] R. L. FRANK, CH. HAINZL, B. SCHLEIN AND R. SEIRINGER, *Time-dependent Bogolubov-de-Gennes equations and non-validity of Ginzburg-Landau theory*, arXiv preprint arXiv:1504.05885 (2015).
- [22] E. HAIRER, CH. LUBICH AND G. WANNER, *Geometric numerical integration: structure-preserving algorithms for ordinary differential equations*, Springer, Berlin, 2006, 2nd edition.
- [23] M. SUZUKI, *Fractal decomposition of exponential operators with applications to many-body theories and Monte Carlo simulations*, Physics Letters A, 146 (1990), pp. 319-323.
- [24] H. YOSHIDA, *Construction of higher order symplectic integrators*, Physics Letters A, 150 (1990), pp. 262-268.
- [25] CH. HAINZL, E. HAMZA, R. SEIRINGER AND J. P. SOLOVEJ, *The BCS functional for general pair interactions*, Communications in Mathematical Physics, 281 (2008), pp. 349-367.
- [26] E. HAIRER, S. P. NØRSETT AND G. WANNER, *Solving Ordinary Differential Equations I: Nonstiff Problems*, Springer, Berlin, 1993.